A semi-continuous extended kinetic model

2000 J. Phys. A: Math. Gen. 33 3417

(http://iopscience.iop.org/0305-4470/33/17/302)

J. Phys. A: Math. Gen. **33** (2000) 3417–3430. Printed in the UK PII: S0305-4470(00)11723-8

A semi-continuous extended kinetic model

W Koller, F Hanser and F Schürrer

Institut für Theoretische Physik, Technische Universität Graz, Austria

Received 8 February 2000

Abstract. A set of semi-continuous model Boltzmann equations governing the evolution of a three-component gas mixture is presented. The third species is treated as an excited state of the second species. The model takes into account collisional excitation and de-excitation processes as well as the interaction with monochromatic photons. A kinetic equation for photons is coupled with the model Boltzmann equations. Conservation properties are established and an H-theorem is proven. Numerical solutions to simple test cases are provided.

1. Introduction

The standard formulation of the Boltzmann equation [1] describes the evolution of gas particles without internal degrees of freedom. Such internal energy levels, however, play an important role in the field of radiation gas dynamics [2]. In recent years, a kinetic model [3] has been presented to describe the dynamics of a gas comprised of two-level atoms interacting with the radiation field of monochromatic photons. The interaction of the photons with the gas particles is described by means of Einstein coefficients. To establish a consistent kinetic model, in addition, inelastic scattering processes are included in the formalism of Boltzmann-like transport equations.

In a recent paper [4], Garibotti and Spiga consider a kinetic model for a three-species gas mixture, where the third species is an excited state of the second. This model takes into account only inelastic excitation and de-excitation phenomena. Since it is applied to the transport of electrons and neutrons in a background medium, elastic collision terms are neglected. In a radiation gas dynamics application, however, such terms are essential to drive the gas towards kinetic equilibrium.

By combining aspects of both models, one obtains kinetic equations describing the interaction of a three-species gas mixture with photons triggering transitions between the second and the third species. Such a situation is typical for a laser induced thermal acoustics (LITA) experiment [5], where photons (supplied by a strong coherent laser pulse) excite high-frequency acoustic waves.

In this scenario, the internal energy gap can be orders of magnitudes greater than the mean kinetic energy of the gas particles. Therefore, deviations of the distribution functions from local Maxwellians due to de-excitation processes are to be expected. Nevertheless, the evolution of the gas mixture is usually described by means of linearized fluid-dynamic equations [6]. Recently, a kinetic approach to LITA experiments has been presented in the framework of discrete kinetic theory [7].

The aim of this paper is to establish a consistent semi-continuous kinetic model for the description of LITA experiments. This model will include elastic and inelastic scattering terms

0305-4470/00/173417+14$30.00

as well as the interaction with a radiation field. Semi-continuous models [8,9] are obtained by discretizing the speed variable leaving a continuum of possible directions. They are closer to physical reality than discrete velocity models, where only a finite set of different velocities is accounted for [10].

The great advantage of the semi-continuous approach is that collision terms typically contain only sums of integrals over compact domains (parts of the unit sphere). In numerical implementations, these integrals can be treated, e.g. by resorting to an expansion of the distribution functions in terms of spherical harmonics.

The paper is organized as follows. After stating the appropriate continuous kinetic equations in section 2, we provide the semi-continuous kinetic model in section 3. In section 4 we show the conservation laws as well as an H-theorem by investigating the collision terms. Finally, in section 5 we present some numerical results on the evolution of the distribution functions under the impact of a strong laser pulse.

2. Continuous kinetic equations

In this section we provide kinetic equations for a gas mixture composed of three species, namely A, B and B^*, where B^* is an excited state of B. The energy gap between B^* and B is denoted by $\Delta E > 0$. We consider all elastic scattering processes of the form $N + M \rightleftharpoons N + M$ for $N, M = A, B, B^*$ as well as the inelastic interaction (collisional excitation and de-excitation)

$$A + B \rightleftharpoons A + B^*. \tag{1}$$

Furthermore, we assume that transitions between B and its excited state B^* can also be induced by monochromatic photons. Therefore, we include the reactions

$$B + p \rightleftharpoons B^* \qquad B^* + p \rightarrow B + 2p \tag{2}$$

where p denotes a photon with frequency $\nu = \Delta E/h$, (where h is Planck's constant).

By assuming equal mass m of the three species, we express the conservation of energy E and momentum $\boldsymbol{R}$ by binary collisions as

$$2E/m = v'^2 + v_*'^2 = v^2 + v_*^2 \mp \epsilon^2 \tag{3}$$

$$\boldsymbol{R}/m = v'\hat{\boldsymbol{\Omega}}' + v_*'\hat{\boldsymbol{\Omega}}_*' = v\hat{\boldsymbol{\Omega}} + v_*\hat{\boldsymbol{\Omega}}_* \tag{4}$$

where, for the purpose of discretization, we have resorted to a polar decomposition of the velocity variables, $\boldsymbol{v} = v\hat{\boldsymbol{\Omega}}$ with $v = |\boldsymbol{v}|$ and the unit vector $\hat{\boldsymbol{\Omega}} = \boldsymbol{v}/v$. Primed symbols refer to post-collisional quantities. The quantity ϵ equals zero for elastic collisions and is linked with the energy gap ΔE by

$$\Delta E = \frac{m}{2}\epsilon^2 \tag{5}$$

for inelastic collisions. The minus sign in equation (3) refers to an excitation event and the plus sign to a de-excitation event.

We express the post-collisional velocities by means of the sum of the pre-collisional velocities and the unit vector $\hat{\boldsymbol{n}}'$ pointing in the direction of the relative velocity $\boldsymbol{g}' = \boldsymbol{v}' - \boldsymbol{v}_*'$ after collision:

$$\boldsymbol{v}' = \frac{\boldsymbol{R}}{2m} + \frac{g'}{2}\hat{\boldsymbol{n}}' \qquad \boldsymbol{v}_*' = \frac{\boldsymbol{R}}{2m} - \frac{g'}{2}\hat{\boldsymbol{n}}' \tag{6}$$

where the relative speed after collision is given by $g' = g^{\pm} = \sqrt{g^2 \pm 2\epsilon^2}$ in the case of inelastic collisions and by $g' = g$ in the case of elastic collisions. If the post-collisional velocity $\boldsymbol{v}'$ results from an (de-)excitation event, we will denote it by $(\boldsymbol{v}^+)$ $\boldsymbol{v}^-$. The functions

$f \equiv f^A$, $\check{f} \equiv f^B$ and $\hat{f} \equiv f^{B^*}$ describe the phase density of the particles A, B and B^*, respectively. According to [4], the inelastic collision terms read

$$\mathcal{J}[f, \hat{f}, \check{f}] = \int_{\mathbb{R}^3} \mathrm{d}\boldsymbol{v}_* \int_{\mathbb{S}^2} \mathrm{d}\hat{\boldsymbol{n}}'\, g\check{\sigma}(g, \gamma)[f(\boldsymbol{v}^+)\check{f}(\boldsymbol{v}_*^+) - f(\boldsymbol{v})\hat{f}(\boldsymbol{v}_*)] + \int_{\mathbb{R}^3} \mathrm{d}\boldsymbol{v}_* \int_{\mathbb{S}^2} \mathrm{d}\hat{\boldsymbol{n}}'\, g\hat{\sigma}(g, \gamma)[f(\boldsymbol{v}^-)\hat{f}(\boldsymbol{v}_*^-) - f(\boldsymbol{v})\check{f}(\boldsymbol{v}_*)] \tag{7a}$$

$$\check{\mathcal{J}}[f, \hat{f}, \check{f}] = \int_{\mathbb{R}^3} \mathrm{d}\boldsymbol{v}_* \int_{\mathbb{S}^2} \mathrm{d}\hat{\boldsymbol{n}}'\, g\hat{\sigma}(g, \gamma)[\hat{f}(\boldsymbol{v}^-)f(\boldsymbol{v}_*^-) - \check{f}(\boldsymbol{v})f(\boldsymbol{v}_*)] \tag{7b}$$

$$\hat{\mathcal{J}}[f, \hat{f}, \check{f}] = \int_{\mathbb{R}^3} \mathrm{d}\boldsymbol{v}_* \int_{\mathbb{S}^2} \mathrm{d}\hat{\boldsymbol{n}}'\, g\check{\sigma}(g, \gamma)[\check{f}(\boldsymbol{v}^+)f(\boldsymbol{v}_*^+) - \hat{f}(\boldsymbol{v})f(\boldsymbol{v}_*)] \tag{7c}$$

with $\cos\gamma = \hat{\boldsymbol{n}} \cdot \hat{\boldsymbol{n}}'$. The microreversibility condition [4] linking the up ($\hat{\sigma}$) and down ($\check{\sigma}$) scattering cross section is given by

$$g^2\hat{\sigma}(g, \gamma) = \Theta(g - \sqrt{2}\epsilon)(g^-)^2\check{\sigma}(g^-, \gamma) \qquad \text{and} \qquad g^2\check{\sigma}(g, \gamma) = (g^+)^2\hat{\sigma}(g^+, \gamma) \tag{8}$$

where Θ is the unit step function. The collision terms describing the impact of elastic scattering between particles N and M on the evolution of N are of the form

$$J^{NM} = \int_{\mathbb{R}^3} \mathrm{d}\boldsymbol{v}_* \int_{\mathbb{S}^2} \mathrm{d}\hat{\boldsymbol{n}}'\, g\sigma(g, \gamma)[f^N(\boldsymbol{v}')f^M(\boldsymbol{v}_*') - f^N(\boldsymbol{v})f^M(\boldsymbol{v}_*)] \tag{9}$$

with the elastic cross section σ. These terms constitute the right-hand side of the continuous Boltzmann equations of the model

$$\frac{\partial f}{\partial t} + v\hat{\boldsymbol{\Omega}} \cdot \frac{\partial f}{\partial \boldsymbol{x}} = \mathcal{J} + J^{AA} + J^{AB} + J^{AB^*} \tag{10a}$$

$$\frac{\partial \check{f}}{\partial t} + v\hat{\boldsymbol{\Omega}} \cdot \frac{\partial \check{f}}{\partial \boldsymbol{x}} = \check{\mathcal{J}} - \mathcal{R}(I) + J^{BB} + J^{BA} + J^{BB^*} \tag{10b}$$

$$\frac{\partial \hat{f}}{\partial t} + v\hat{\boldsymbol{\Omega}} \cdot \frac{\partial \hat{f}}{\partial \boldsymbol{x}} = \hat{\mathcal{J}} + \mathcal{R}(I) + J^{B^*B^*} + J^{B^*A} + J^{B^*B}. \tag{10c}$$

The interaction with monochromatic photons of intensity I is modelled by means of Einstein coefficients α (for spontaneous emission) and β (for absorption and stimulated emission). Neglecting the Doppler effect, the photon–particle interaction term reads

$$\mathcal{R}(I) = \int_{\mathbb{S}^2} \mathrm{d}\hat{\boldsymbol{\Omega}}_*(\beta I(\hat{\boldsymbol{\Omega}}_*)\check{f}(\boldsymbol{v}) - (\alpha + \beta I(\hat{\boldsymbol{\Omega}}_*))\hat{f}(\boldsymbol{v})) \tag{11}$$

where I denotes the specific intensity of photons with energy ΔE. The evolution equation for the specific intensity $I(t, \boldsymbol{x}, \hat{\boldsymbol{\Omega}})$ is given by [2]

$$\frac{\partial I}{\partial t} + c\hat{\boldsymbol{\Omega}} \cdot \frac{\partial I}{\partial \boldsymbol{x}} = \frac{\partial I_L}{\partial t} - c\Delta E \int_{\mathbb{R}^3} \mathrm{d}\boldsymbol{v}(\beta I \check{f}(\boldsymbol{v}) - (\alpha + \beta I)\hat{f}(\boldsymbol{v})) \tag{12}$$

where c stands for the speed of light and $I_L(t, \boldsymbol{x}, \hat{\boldsymbol{\Omega}})$ is the intensity profile of the light sources. The energy density e_ν, the energy flux $\boldsymbol{Q}_\nu$, and the energy density $\mathcal{S}_L$ of the light source are respectively defined by

$$e_\nu = \frac{1}{c}\int_{\mathbb{S}^2} I(\hat{\boldsymbol{\Omega}})\,\mathrm{d}\hat{\boldsymbol{\Omega}} \qquad \boldsymbol{Q}_\nu = \int_{\mathbb{S}^2} \hat{\boldsymbol{\Omega}} I(\hat{\boldsymbol{\Omega}})\,\mathrm{d}\hat{\boldsymbol{\Omega}} \qquad \mathcal{S}_L = \frac{1}{c}\int_{\mathbb{S}^2} I_L(\hat{\boldsymbol{\Omega}})\,\mathrm{d}\hat{\boldsymbol{\Omega}}. \tag{13}$$

The conservation of mass, momentum and energy as well as an H-theorem for the inelastic collision terms of the above sketched model are provided in [4]. A derivation of Planck's law of radiation and an H-function for the photon transport equation can be found in [3].

3. Semi-continuous kinetic model

The kinetic equations describing the evolution of the gas mixture and the photon intensity are constituted by equations (10*a*)–(10*c*) and (12). In order to discretize them, we apply a generalized form of the procedure introduced by Preziosi and Longo. In [9], the authors derive semi-continuous kinetic equations for a single species of a monatomic gas by discretizing the speed variable in an appropriate manner.

Following their lines, as a first step we restrict the range of the particle's kinetic energies to the interval $I_v = [E_m, E_M)$, $0 < E_m < E_M < \infty$. The bounds of I_v are to be chosen such that all particles with kinetic energies outside of I_v may be neglected. Next we introduce an arithmetical sequence of energies

$$E_i = E_m + (i + \tfrac{1}{2})\delta \qquad i = 0, 1, \ldots, n \tag{14}$$

with $\delta = 2(E_M - E_m)/(n + 1)$ that are the centres of the subintervals (energy groups)

$$I_i = \left[E_i - \frac{\delta}{2}, E_i + \frac{\delta}{2}\right] \qquad i = 0, 1, \ldots, n. \tag{15}$$

Furthermore, we have to adapt the energy gap ΔE in such a way that it fits into the discretization scheme. Therefore we set $\Delta E = q\delta$ with $q \in \{1, 2, \ldots, 2n - 1\}$ which implies $\epsilon^2 = 2q\delta/m$. When appearing as an integrand, any function of kinetic energy (and thus of the speed v) will henceforth be approximated by a piecewise constant interpolant defined over the above-stated discretization:

$$g(E) \approx \sum_{i=0}^{n} g_i \chi_{I_i}(E) \tag{16}$$

where $\chi_B(.)$ denotes the characteristic function of the set B.

Each energy knot E_i corresponds to a speed $v_i = \sqrt{2E_i/m}$. Using this discrete set of allowed speeds, we tackle the question which solid angles are compatible with a chosen pair of pre-collisional (v, v_*) and post-collisional (v', v'_*) speeds that satisfy the conservation of energy. The combination of conservation of momentum and total energy, i.e. equations (3) and (4), yields

$$2v'v'_*\hat{\boldsymbol{\Omega}}' \cdot \hat{\boldsymbol{\Omega}}'_* = 2vv_*\hat{\boldsymbol{\Omega}} \cdot \hat{\boldsymbol{\Omega}}_* \pm \epsilon^2. \tag{17}$$

Now the inequality $|\hat{\boldsymbol{\Omega}}' \cdot \hat{\boldsymbol{\Omega}}'_*| \leqslant 1$ implies that when fixing $\hat{\boldsymbol{\Omega}}$, the variation of the solid angle $\hat{\boldsymbol{\Omega}}_*$ is restricted to

$$\begin{pmatrix} \hat{D}_* \\ \check{D}_* \end{pmatrix} = \left\{ \hat{\boldsymbol{\Omega}}_* \in \mathbb{S}^2 \,\middle|\, -\frac{v'v'_*}{vv_*} \mp \frac{\epsilon^2}{2vv_*} \leqslant \hat{\boldsymbol{\Omega}} \cdot \hat{\boldsymbol{\Omega}}_* \leqslant \frac{v'v'_*}{vv_*} \mp \frac{\epsilon^2}{2vv_*} \right\}. \tag{18}$$

Figure 1 shows a graphical representation of these sets. For elastic collisions ($\epsilon = 0$), the inner product $\hat{\boldsymbol{\Omega}} \cdot \hat{\boldsymbol{\Omega}}_*$ is symmetric with respect to zero. In this case we define $D_* = \hat{D}_* = \check{D}_*$. For inelastic excitation ($\hat{D}_*$) and de-excitation ($\check{D}_*$) processes this is no longer true.

Furthermore, by introducing the angle ϑ between the pre-collisional and post-collisional plane spanned by the pairs $(\boldsymbol{g}, \boldsymbol{R})$ and $(\boldsymbol{g}', \boldsymbol{R})$, respectively, the surface element $\mathrm{d}\hat{\boldsymbol{n}}'$ appearing in the collision terms can be written as [9]

$$\mathrm{d}\hat{\boldsymbol{n}}' = \frac{4}{g'R} v' \,\mathrm{d}v' \,\mathrm{d}\vartheta. \tag{19}$$

Now, we integrate equations (7*a*)–(7*c*) over one energy interval I_i with the appropriate measure $\sqrt{2E/m^3}\,\mathrm{d}E = v^2\,\mathrm{d}v$ and approximate all functions of kinetic energy by piecewise constant interpolants (cf remark 3.4 in [9]). By following the considerations of section 4

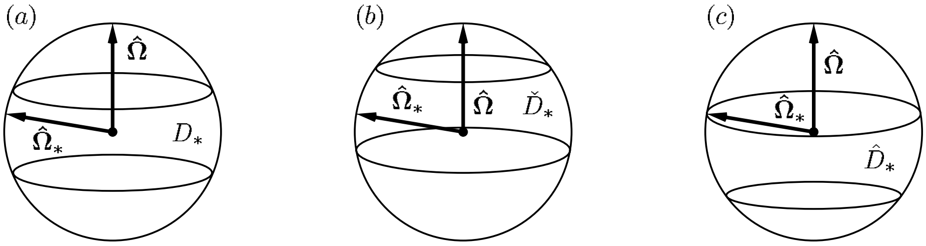

Figure 1. Domains of $\hat{\mathbf{\Omega}}_*$ as implied by the conservation of momentum for elastic scattering (*a*), collisional de-excitation (*b*), and collisional excitation (*c*).

in [9], we obtain semi-continuous versions of the inelastic collision terms. If the cross section is independent of the scattering angle, which we shall assume for simplicity, they read

$$\mathcal{J}_i[f, \check{f}, \hat{f}] = C_\chi^2 \sum_{j=0}^{n} v_j \sum_{\substack{h,k=0 \\ h+k=i+j+q}}^{n} \int_0^{2\pi} \mathrm{d}\vartheta \int_{\check{D}_*(v_i,v_j,v_h)} \mathrm{d}\hat{\mathbf{\Omega}}_* \check{A}_{ij}^{hk}(\hat{\mathbf{\Omega}}\cdot\hat{\mathbf{\Omega}}_*)(f_h' \check{f}_{*k}' - f_i \hat{f}_{*j})$$
$$+ C_\chi^2 \sum_{j=0}^{n} v_j \sum_{\substack{h,k=0 \\ h+k=i+j-q}}^{n} \int_0^{2\pi} \mathrm{d}\vartheta \int_{\hat{D}_*(v_i,v_j,v_h)} \mathrm{d}\hat{\mathbf{\Omega}}_* \hat{A}_{ij}^{hk}(\hat{\mathbf{\Omega}}\cdot\hat{\mathbf{\Omega}}_*)(f_h' \hat{f}_{*k}' - f_i \check{f}_{*j}) \tag{20a}$$

$$\check{\mathcal{J}}_i[f, \check{f}, \hat{f}] = C_\chi^2 \sum_{j=0}^{n} v_j \sum_{\substack{h,k=0 \\ h+k=i+j-q}}^{n} \int_0^{2\pi} \mathrm{d}\vartheta \int_{\hat{D}_*(v_i,v_j,v_h)} \mathrm{d}\hat{\mathbf{\Omega}}_* \hat{A}_{ij}^{hk}(\hat{\mathbf{\Omega}}\cdot\hat{\mathbf{\Omega}}_*)(\hat{f}_h' f_{*k}' - \check{f}_i f_{*j}) \tag{20b}$$

$$\hat{\mathcal{J}}_i[f, \check{f}, \hat{f}] = C_\chi^2 \sum_{j=0}^{n} v_j \sum_{\substack{h,k=0 \\ h+k=i+j+q}}^{n} \int_0^{2\pi} \mathrm{d}\vartheta \int_{\check{D}_*(v_i,v_j,v_h)} \mathrm{d}\hat{\mathbf{\Omega}}_* \check{A}_{ij}^{hk}(\hat{\mathbf{\Omega}}\cdot\hat{\mathbf{\Omega}}_*)(\check{f}_h' f_{*k}' - \hat{f}_i f_{*j}) \tag{20c}$$

where $C_\chi = \delta/m$. The application of the same strategy to the elastic collision terms, i.e. equation (9), yields

$$J_i^{NM}[f^N, f^M] = C_\chi^2 \sum_{j=0}^{n} v_j \sum_{\substack{h,k=0 \\ h+k=i+j}}^{n} \int_0^{2\pi} \mathrm{d}\vartheta \int_{D_*(v_i,v_j,v_h)} \mathrm{d}\hat{\mathbf{\Omega}}_* A_{ij}^{hk}(\hat{\mathbf{\Omega}}\cdot\hat{\mathbf{\Omega}}_*)(f_h^{N\prime} f_{*k}^{M\prime} - f_i^N f_{*j}^M) \tag{21}$$

for $N, M = A, B, B^*$. The domain $\hat{D}_*(v_i, v_j, v_h)$ takes into account the threshold $g \geqslant \sqrt{2}\epsilon$ for collisional excitations. We have used the shorthand notations

$$f_i^N = f_i^N(\hat{\mathbf{\Omega}}) = f^N(v_i\hat{\mathbf{\Omega}}) \qquad f_{*j}^N = f_j^N(\hat{\mathbf{\Omega}}_*) = f^N(v_j\hat{\mathbf{\Omega}}_*)$$
$$f_h^{N\prime} = f_h^N(\hat{\mathbf{\Omega}}') = f^N(v_h\hat{\mathbf{\Omega}}') \qquad f_{*k}^{N\prime} = f_k^N(\hat{\mathbf{\Omega}}_*') = f^N(v_k\hat{\mathbf{\Omega}}_*') \tag{22}$$

where $N = A, B, B^*$. Post-collisional solid angles are functions of pre-collisional solid angles, of the speeds v_i, v_j, and v_h and of the angle ϑ. The kernels are given by

$$A_{ij}^{hk}(\hat{\mathbf{\Omega}}\cdot\hat{\mathbf{\Omega}}_*) = \frac{4\sigma(g)}{R} \qquad \hat{A}_{ij}^{hk}(\hat{\mathbf{\Omega}}\cdot\hat{\mathbf{\Omega}}_*) = \frac{4g}{g^-}\frac{\hat{\sigma}(g)}{R} \qquad \check{A}_{ij}^{hk}(\hat{\mathbf{\Omega}}\cdot\hat{\mathbf{\Omega}}_*) = \frac{4g}{g^+}\frac{\check{\sigma}(g)}{R}. \tag{23}$$

In these formulae, the quantities g, $g^\pm$ and R have to be evaluated at the speed knots,

$$g = \sqrt{v_i^2 + v_j^2 - 2v_i v_j \hat{\mathbf{\Omega}}\cdot\hat{\mathbf{\Omega}}_*} \qquad R = \sqrt{v_i^2 + v_j^2 + 2v_i v_j \hat{\mathbf{\Omega}}\cdot\hat{\mathbf{\Omega}}_*} \tag{24}$$

and so on for g^+ and g^-. By applying the same strategy to the streaming part of the Boltzmann equations and equating the result to the above-stated collision terms, we obtain the semi-continuous kinetic equations

$$\frac{\partial f_i}{\partial t} + v_i \hat{\boldsymbol{\Omega}} \frac{\partial f_i}{\partial \boldsymbol{x}} = \mathcal{J}_i + J_i^{AA} + J_i^{AB} + J_i^{AB^*} \tag{25a}$$

$$\frac{\partial \check{f}_i}{\partial t} + v_i \hat{\boldsymbol{\Omega}} \frac{\partial \check{f}_i}{\partial \boldsymbol{x}} = \check{\mathcal{J}}_i - \mathcal{R}_i(I) + J_i^{BB} + J_i^{BA} + J_i^{BB^*} \tag{25b}$$

$$\frac{\partial \hat{f}_i}{\partial t} + v_i \hat{\boldsymbol{\Omega}} \frac{\partial \hat{f}_i}{\partial \boldsymbol{x}} = \hat{\mathcal{J}}_i + \mathcal{R}_i(I) + J_i^{B^*B^*} + J_i^{B^*A} + J_i^{B^*B} \tag{25c}$$

with $\mathcal{R}_i(I)$ being defined as equation (11) evaluated at the speed knot i, i.e. for $\check{f}_i(\hat{\boldsymbol{\Omega}})$ and $\hat{f}_i(\hat{\boldsymbol{\Omega}})$. The photon transport equation now reads

$$\frac{\partial I}{\partial t} + c\hat{\boldsymbol{\Omega}} \cdot \frac{\partial I}{\partial \boldsymbol{x}} = \frac{\partial I_L}{\partial t} - c\Delta E(\beta I \check{n} - (\alpha + \beta I)\hat{n}). \tag{26}$$

In the semi-continuous formulation, the macroscopic quantities of each species N, namely particle density, the mean velocity, the momentum flux, and the kinetic energy flux are respectively given by

$$n^N = C_\chi \sum_{i=0}^{n} v_i \int_{\mathbb{S}^2} f_i^N(\hat{\boldsymbol{\Omega}})\,\mathrm{d}\hat{\boldsymbol{\Omega}} \tag{27a}$$

$$\boldsymbol{u}^N = \frac{C_\chi}{n^N} \sum_{i=0}^{n} v_i^2 \int_{\mathbb{S}^2} \hat{\boldsymbol{\Omega}} f_i^N(\hat{\boldsymbol{\Omega}})\,\mathrm{d}\hat{\boldsymbol{\Omega}} \tag{27b}$$

$$\mathbb{K}^N = C_\chi m \sum_{i=0}^{n} v_i^3 \int_{\mathbb{S}^2} \hat{\boldsymbol{\Omega}} \otimes \hat{\boldsymbol{\Omega}} f_i^N(\hat{\boldsymbol{\Omega}})\,\mathrm{d}\hat{\boldsymbol{\Omega}} \tag{27c}$$

$$\boldsymbol{Q}^N = \frac{C_\chi m}{2} \sum_{i=0}^{n} v_i^4 \int_{\mathbb{S}^2} \hat{\boldsymbol{\Omega}} f_i^N(\hat{\boldsymbol{\Omega}})\,\mathrm{d}\hat{\boldsymbol{\Omega}}. \tag{27d}$$

The kinetic energy density of species N is given by the trace $k^N = (1/2)\,\mathrm{tr}\,\mathbb{K}^N$. The total energy density e of the gas is the sum of the kinetic energy densities plus the internal energy density of B^*:

$$e = k^A + k^B + k^{B^*} + n^{B^*}\Delta E. \tag{28}$$

By using these definitions, we can integrate equations (25*a*)–(25*c*) and (26) to obtain the macroscopic equations for the semi-continuous model:

$$\frac{\partial n}{\partial t} + \frac{\partial}{\partial \boldsymbol{x}} \cdot (n\boldsymbol{u}) = 0 \tag{29a}$$

$$\frac{\partial}{\partial t}(\check{n} + \hat{n}) + \frac{\partial}{\partial \boldsymbol{x}} \cdot (\check{n}\check{\boldsymbol{u}} + \hat{n}\hat{\boldsymbol{u}}) = 0 \tag{29b}$$

$$m\frac{\partial}{\partial t}(\check{n}\check{\boldsymbol{u}} + \hat{n}\hat{\boldsymbol{u}} + n\boldsymbol{u}) + \frac{\partial}{\partial \boldsymbol{x}} \cdot (\mathbb{K} + \check{\mathbb{K}} + \hat{\mathbb{K}}) = 0 \tag{29c}$$

$$\frac{\partial}{\partial t}(e + e_\nu) + \frac{\partial}{\partial \boldsymbol{x}} \cdot (\boldsymbol{Q} + \check{\boldsymbol{Q}} + \hat{\boldsymbol{Q}} + \boldsymbol{Q}_\nu) = \frac{\partial S_L}{\partial t}. \tag{29d}$$

They reflect the conservation of particles A, B plus B^*, the conservation of total momentum and injection of energy due to external light sources. The proof of these macroscopic equations involves important properties of the collision terms and is presented in the following section.

4. Properties of the semi-continuous collision terms

We will now summarize some major aspects of binary collisions in a semi-continuous velocity space (cf [9]). First of all, the microreversibility conditions for inelastic scattering, i.e. equations (8) imply the identities

$$\check{A}^{ij}_{hk}(\hat{\mathbf{\Omega}}' \cdot \hat{\mathbf{\Omega}}'_*) = \hat{A}^{hk}_{ij}(\hat{\mathbf{\Omega}} \cdot \hat{\mathbf{\Omega}}_*) \qquad \hat{A}^{ij}_{hk}(\hat{\mathbf{\Omega}}' \cdot \hat{\mathbf{\Omega}}'_*) = \check{A}^{hk}_{ij}(\hat{\mathbf{\Omega}} \cdot \hat{\mathbf{\Omega}}_*) \tag{30}$$

that are generalizations of the relation valid for the elastic kernels:

$$A^{ij}_{hk}(\hat{\mathbf{\Omega}}' \cdot \hat{\mathbf{\Omega}}'_*) = A^{hk}_{ij}(\hat{\mathbf{\Omega}} \cdot \hat{\mathbf{\Omega}}_*). \tag{31}$$

Equations (30) and (31) constitute the appropriate microreversibility conditions for the semi-continuous model. Furthermore, the symmetry properties

$$A^{hk}_{ij}(\hat{\mathbf{\Omega}} \cdot \hat{\mathbf{\Omega}}_*) = A^{kh}_{ji}(\hat{\mathbf{\Omega}}_* \cdot \hat{\mathbf{\Omega}}) \tag{32}$$

are also valid in the inelastic case, i.e. for $\check{A}^{hk}_{ij}$ and $\hat{A}^{hk}_{ij}$.

For fixed speeds v, v_*, v' and v'_* and for a fixed angle ϑ between the pre- and post-collisional plane, collisional de-excitations map the solid angles $(\hat{\mathbf{\Omega}}, \hat{\mathbf{\Omega}}_*) \in \mathbb{S}^2 \times \check{D}_*(v, v_*, v')$ to $(\hat{\mathbf{\Omega}}', \hat{\mathbf{\Omega}}'_*) \in \mathbb{S}^2 \times \hat{D}_*(v', v'_*, v)$. Conversely, excitation events relate $(\hat{\mathbf{\Omega}}, \hat{\mathbf{\Omega}}_*) \in \mathbb{S}^2 \times \hat{D}_*(v, v_*, v')$ to $(\hat{\mathbf{\Omega}}', \hat{\mathbf{\Omega}}'_*) \in \mathbb{S}^2 \times \check{D}_*(v', v'_*, v)$. Due to microreversibility, these maps are bijections. The Jacobian of these maps for both elastic and inelastic collisions is given by

$$\frac{\partial(\hat{\mathbf{\Omega}}', \hat{\mathbf{\Omega}}'_*)}{\partial(\hat{\mathbf{\Omega}}, \hat{\mathbf{\Omega}}_*)} = \frac{v v_*}{v' v'_*}. \tag{33}$$

For elastic collisions, the proof of this relation is given in [9]. Since this proof mainly involves the conservation of momentum that is valid also for inelastic collisions, we refer to proposition 2.4 in [9] and skip the repetition of the proof here.

For a set of arbitrary functions $\varphi^N_i(\hat{\mathbf{\Omega}})$, $N = A, B, B^*$ we introduce the notation

$$\langle \varphi^N, f^N \rangle = C_\chi \sum_{i=0}^{n} v_i \int_{\mathbb{S}^2} \mathrm{d}\hat{\mathbf{\Omega}}\, \varphi^N_i(\hat{\mathbf{\Omega}}) f^N_i(\hat{\mathbf{\Omega}}).$$

Now we can state the main properties of the model. First, the expression

$$\begin{aligned}\langle\langle \varphi, \boldsymbol{J} \rangle\rangle \equiv\ & \langle \varphi, \mathcal{J} + J^{AA} + J^{AB} + J^{AB^*} \rangle \\ & + \langle \check{\varphi}, \check{\mathcal{J}} + J^{BB} + J^{BA} + J^{BB^*} \rangle + \langle \hat{\varphi}, \hat{\mathcal{J}} + J^{B^*B^*} + J^{B^*A} + J^{B^*B} \rangle \end{aligned} \tag{34}$$

vanishes for the choices $\varphi_i = 1, \check{\varphi}_i = \hat{\varphi}_i = 0$; $\varphi_i = 0, \check{\varphi}_i = \hat{\varphi}_i = 1$; $\varphi_i = \check{\varphi}_i = \hat{\varphi}_i = v_i \hat{\mathbf{\Omega}}$ and $\varphi_i = \check{\varphi}_i = v_i^2, \hat{\varphi}_i = v_i^2 + \epsilon^2$. They correspond to the conservation and balance equations stated in equations (29*a*)–(29*d*). Furthermore, we obtain a space homogeneous H-theorem by setting $\varphi^N_i = \log f^N_i$. It reads

$$\frac{\partial H}{\partial t} \equiv \langle\langle \log f, \boldsymbol{J} \rangle\rangle \leqslant 0. \tag{35}$$

This H-function is zero (collisional equilibrium of the gas mixture) if and only if

$$f^N_i(\hat{\mathbf{\Omega}}) = A^N \exp(v_i \boldsymbol{b} \cdot \hat{\mathbf{\Omega}} - c v_i^2) \tag{36}$$

with the constants A^N, $\boldsymbol{b}$, and $c = m/(2k_{\mathrm{B}}T)$, where T is the temperature and k_{B} denotes Boltzmann's constant. The ratio between the densities of B^* and B reads

$$\frac{\hat{n}}{\check{n}} = \exp\left(-\frac{\Delta E}{k_{\mathrm{B}} T}\right) \tag{37}$$

which is exactly Boltzmann's formula. Finally, in the absence of external light sources, the equilibrium intensity is given by Planck's law [3]

$$I = \frac{\alpha/\beta}{\exp(\Delta E/(k_\mathrm{B}T)) - 1}. \tag{38}$$

Since the bracket $\langle \varphi, f \rangle$ is linear in its second argument, we can discuss the various terms in equation (34) separately. We start with the discussion of the elastic collision terms J^{NM}. For an arbitrary set of functions $\varphi_i^N(\hat{\mathbf{\Omega}})$ we obtain by exchanging $i \leftrightarrow h$, $\hat{\mathbf{\Omega}} \leftrightarrow \hat{\mathbf{\Omega}}'$ and $j \leftrightarrow k$, $\hat{\mathbf{\Omega}}_* \leftrightarrow \hat{\mathbf{\Omega}}'_*$ in the gain term, applying equation (31) and transforming back to pre-collisional solid angles using equation (33)

$$\langle \varphi^N, J^{NM} \rangle = C_\chi^3 \sum_{\substack{i,j,h,k=0\\ h+k=i+j}}^{n} v_i v_j \int_0^{2\pi} \mathrm{d}\vartheta \iint_{\mathbb{S}^2 \times D_*(v_i,v_j,v_h)} \mathrm{d}\hat{\mathbf{\Omega}}\, \mathrm{d}\hat{\mathbf{\Omega}}_*\, A_{ij}^{hk}(\hat{\mathbf{\Omega}} \cdot \hat{\mathbf{\Omega}}_*)$$
$$\times f_i^N(\hat{\mathbf{\Omega}}) f_j^M(\hat{\mathbf{\Omega}}_*)(\varphi_h^N(\hat{\mathbf{\Omega}}') - \varphi_i^N(\hat{\mathbf{\Omega}})) \tag{39}$$

which for $\varphi_i^N(\hat{\mathbf{\Omega}}) = 1$ immediately shows the conservation of the particles N. The conservation of momentum and energy is implied by

$$\langle \varphi^N, J^{NM} \rangle + \langle \varphi^M, J^{MN} \rangle = 0 \tag{40}$$

which is valid for $\varphi_i^N(\hat{\mathbf{\Omega}}) = \varphi_i^M(\hat{\mathbf{\Omega}}) = v_i\hat{\mathbf{\Omega}}$ and $\varphi_i^N(\hat{\mathbf{\Omega}}) = \varphi_i^M(\hat{\mathbf{\Omega}}) = v_i^2$, respectively. This can be seen by exchanging $i \leftrightarrow j$, $\hat{\mathbf{\Omega}} \leftrightarrow \hat{\mathbf{\Omega}}_*$ and $h \leftrightarrow k$, $\hat{\mathbf{\Omega}}' \leftrightarrow \hat{\mathbf{\Omega}}'_*$ in the second term of equation (40), applying the symmetry property (32) and taking into account detailed conservation of momentum and energy.

For the space homogeneous case, an H-functional is derived by setting $\varphi_i^N(\hat{\mathbf{\Omega}}) = \log f_i^N(\hat{\mathbf{\Omega}})$ and performing the same changes in the second term of equation (40). By exchanging pre- and post-collisional quantities and transforming back the integrals using equation (33), we can symmetrize the result to obtain

$$\dot{H}^{NM} = \langle \log f^N, J^{NM} \rangle + \langle \log f^M, J^{MN} \rangle$$
$$= \frac{C_\chi^3}{2} \sum_{\substack{i,j,h,k=0\\ h+k=i+j}}^{n} v_i v_j \int_0^{2\pi} \mathrm{d}\vartheta \iint_{\mathbb{S}^2 \times D(v_i,v_j,v_h)} \mathrm{d}\hat{\mathbf{\Omega}}\, \mathrm{d}\hat{\mathbf{\Omega}}_* A_{ij}^{hk}(\hat{\mathbf{\Omega}} \cdot \hat{\mathbf{\Omega}}_*)$$
$$\times (f_i^N(\hat{\mathbf{\Omega}}) f_j^M(\hat{\mathbf{\Omega}}_*) - f_h^N(\hat{\mathbf{\Omega}}') f_k^M(\hat{\mathbf{\Omega}}'_*)) \log\left(\frac{\varphi_h^N(\hat{\mathbf{\Omega}}')\varphi_k^M(\hat{\mathbf{\Omega}}'_*)}{\varphi_i^N(\hat{\mathbf{\Omega}})\varphi_j^M(\hat{\mathbf{\Omega}}_*)}\right)$$
$$\leqslant 0. \tag{41}$$

For collisional equilibrium, we first refer to theorem 5.2 of [9] that states that the equal sign applies in $\dot{H}^{NN} \leqslant 0$ if and only if $f_i^N(\hat{\mathbf{\Omega}})$ is a Maxwellian of the form

$$f_i^N(\hat{\mathbf{\Omega}}) = A^N \exp(v_i \boldsymbol{b}^N \cdot \hat{\mathbf{\Omega}} - c^N v_i^2) \tag{42}$$

with parameters A^N, $\boldsymbol{b}^N$, and c^N. The further condition $\dot{H}^{NM} = 0$ is fulfilled if and only if additionally $\boldsymbol{b}^N = \boldsymbol{b}^M$ and $c^N = c^M$. As in continuous kinetic theory, the elastic collision terms of the mixture ensure equal drift velocity and temperature for all species in equilibrium.

Now we treat the brackets involving the inelastic collision integrals. For arbitrary functions $\varphi_i(\hat{\mathbf{\Omega}})$, $\hat{\varphi}_i(\hat{\mathbf{\Omega}})$ and $\check{\varphi}_i(\hat{\mathbf{\Omega}})$, by means of the same manipulations we obtain

$$\langle \varphi, \mathcal{J} \rangle = C_\chi^3 \sum_{\substack{i,j,h,k=0\\ h+k=i+j+q}}^{n} v_i v_j \int_0^{2\pi} \mathrm{d}\vartheta$$

$$\times \iint_{\mathbb{S}^2\times\check{D}_*(v_i,v_j,v_h)} \mathrm{d}\hat{\mathbf{\Omega}}\,\mathrm{d}\hat{\mathbf{\Omega}}_*\check{A}_{ij}^{hk}(\hat{\mathbf{\Omega}}\cdot\hat{\mathbf{\Omega}}_*)f_i(\hat{\mathbf{\Omega}})\hat{f}_j(\hat{\mathbf{\Omega}}_*)(\varphi_h(\hat{\mathbf{\Omega}}')-\varphi_i(\hat{\mathbf{\Omega}}))$$

$$+C_\chi^3 \sum_{\substack{i,j,h,k=0\\h+k=i+j-q}}^{n} v_i v_j \int_0^{2\pi}\mathrm{d}\vartheta$$

$$\times \iint_{\mathbb{S}^2\times\hat{D}_*(v_i,v_j,v_h)} \mathrm{d}\hat{\mathbf{\Omega}}\,\mathrm{d}\hat{\mathbf{\Omega}}_*\hat{A}_{ij}^{hk}(\hat{\mathbf{\Omega}}\cdot\hat{\mathbf{\Omega}}_*)f_i(\hat{\mathbf{\Omega}})\check{f}_j(\hat{\mathbf{\Omega}}_*)(\varphi_h(\hat{\mathbf{\Omega}}')-\varphi_i(\hat{\mathbf{\Omega}})) \qquad (43a)$$

$$\langle\check{\varphi},\check{\mathcal{J}}\rangle = C_\chi^3 \sum_{\substack{i,j,h,k=0\\h+k=i+j+q}}^{n} v_i v_j \int_0^{2\pi}\mathrm{d}\vartheta$$

$$\times \iint_{\mathbb{S}^2\times\check{D}_*(v_i,v_j,v_h)} \mathrm{d}\hat{\mathbf{\Omega}}\,\mathrm{d}\hat{\mathbf{\Omega}}_*\check{A}_{ij}^{hk}(\hat{\mathbf{\Omega}}\cdot\hat{\mathbf{\Omega}}_*)\check{\varphi}_k(\hat{\mathbf{\Omega}}'_*)\hat{f}_j(\hat{\mathbf{\Omega}}_*)f_i(\hat{\mathbf{\Omega}})$$

$$-C_\chi^3 \sum_{\substack{i,j,h,k=0\\h+k=i+j-q}}^{n} v_i v_j \int_0^{2\pi}\mathrm{d}\vartheta$$

$$\times \iint_{\mathbb{S}^2\times\hat{D}_*(v_i,v_j,v_h)} \mathrm{d}\hat{\mathbf{\Omega}}\,\mathrm{d}\hat{\mathbf{\Omega}}_*\hat{A}_{ij}^{hk}(\hat{\mathbf{\Omega}}\cdot\hat{\mathbf{\Omega}}_*)\check{\varphi}_j(\hat{\mathbf{\Omega}}_*)\check{f}_j(\hat{\mathbf{\Omega}}_*)f_i(\hat{\mathbf{\Omega}}) \qquad (43b)$$

$$\langle\hat{\varphi},\hat{\mathcal{J}}\rangle = C_\chi^3 \sum_{\substack{i,j,h,k=0\\h+k=i+j-q}}^{n} v_i v_j \int_0^{2\pi}\mathrm{d}\vartheta$$

$$\times \iint_{\mathbb{S}^2\times\hat{D}_*(v_i,v_j,v_h)} \mathrm{d}\hat{\mathbf{\Omega}}\,\mathrm{d}\hat{\mathbf{\Omega}}_*\hat{A}_{ij}^{hk}(\hat{\mathbf{\Omega}}\cdot\hat{\mathbf{\Omega}}_*)\hat{\varphi}_k(\hat{\mathbf{\Omega}}'_*)\check{f}_j(\hat{\mathbf{\Omega}}_*)f_i(\hat{\mathbf{\Omega}})$$

$$-C_\chi^3 \sum_{\substack{i,j,h,k=0\\h+k=i+j+q}}^{n} v_i v_j \int_0^{2\pi}\mathrm{d}\vartheta$$

$$\times \iint_{\mathbb{S}^2\times\check{D}_*(v_i,v_j,v_h)} \mathrm{d}\hat{\mathbf{\Omega}}\,\mathrm{d}\hat{\mathbf{\Omega}}_*\check{A}_{ij}^{hk}(\hat{\mathbf{\Omega}}\cdot\hat{\mathbf{\Omega}}_*)\hat{\varphi}_j(\hat{\mathbf{\Omega}}_*)\hat{f}_j(\hat{\mathbf{\Omega}}_*)f_i(\hat{\mathbf{\Omega}}). \qquad (43c)$$

In equations (43*b*) and (43*c*), we have additionally exchanged the indices $i \leftrightarrow j$ and $h \leftrightarrow k$ as well as $\hat{\mathbf{\Omega}} \leftrightarrow \hat{\mathbf{\Omega}}_*$, $\hat{\mathbf{\Omega}}' \leftrightarrow \hat{\mathbf{\Omega}}'_*$ which leaves the expressions unaltered.

Now, equation (43*a*) vanishes for $\varphi_i(\hat{\mathbf{\Omega}}) = 1$ which corresponds to the conservation of particles A. Furthermore, $\langle\check{\varphi},\check{\mathcal{J}}\rangle + \langle\hat{\varphi},\hat{\mathcal{J}}\rangle = 0$ for $\check{\varphi}_i(\hat{\mathbf{\Omega}}) = \hat{\varphi}_i(\hat{\mathbf{\Omega}}) = 1$ which reflects the conservation of the sum of particles B plus B^*.

In order to show the conservation of total momentum, we set $\varphi_i(\hat{\mathbf{\Omega}}) = \check{\varphi}_i(\hat{\mathbf{\Omega}}) = \hat{\varphi}_i(\hat{\mathbf{\Omega}}) = v_i\hat{\mathbf{\Omega}}$. From detailed conservation of momentum and equations (43*a*)–(43*c*) follows

$$\langle\varphi,\mathcal{J}\rangle + \langle\check{\varphi},\check{\mathcal{J}}\rangle + \langle\hat{\varphi},\hat{\mathcal{J}}\rangle = 0. \qquad (44)$$

The same identity holds for $\varphi_i(\hat{\mathbf{\Omega}}) = \check{\varphi}_i(\hat{\mathbf{\Omega}}) = v_i^2$, $\hat{\varphi}_i(\hat{\mathbf{\Omega}}) = v_i^2 + \epsilon^2$ which ensures the conservation of total energy.

We obtain an H-functional by putting $\varphi_i^N(\hat{\mathbf{\Omega}}) = \log f_i^N(\hat{\mathbf{\Omega}})$, $N = A, B, B^*$. In fact, by transforming pre-collisional quantities to post-collisional ones in all terms involving $\hat{A}_{ij}^{hk}(\hat{\mathbf{\Omega}}\cdot\hat{\mathbf{\Omega}}_*)$ in equations (43*a*)–(43*c*) and by consequently eliminating $\hat{A}_{hk}^{ij}(\hat{\mathbf{\Omega}}'\cdot\hat{\mathbf{\Omega}}'_*)$ by means of equation (30) we obtain

$$\dot{\mathcal{H}} \equiv \langle \log f, \mathcal{J} \rangle + \langle \log \check{f}, \check{\mathcal{J}} \rangle + \langle \log \hat{f}, \hat{\mathcal{J}} \rangle$$
$$= C_\chi^3 \sum_{\substack{i,j,h,k=0 \\ h+k=i+j+q}}^{n} v_i v_j \int_0^{2\pi} \mathrm{d}\vartheta \iint_{\mathbb{S}^2 \times \check{D}_*(v_i,v_j,v_h)} \mathrm{d}\hat{\boldsymbol{\Omega}}\, \mathrm{d}\hat{\boldsymbol{\Omega}}_* \check{A}_{ij}^{hk}(\hat{\boldsymbol{\Omega}} \cdot \hat{\boldsymbol{\Omega}}_*)$$
$$\times (f_i(\hat{\boldsymbol{\Omega}}) \hat{f}_j(\hat{\boldsymbol{\Omega}}_*) - f_h(\hat{\boldsymbol{\Omega}}_*) \check{f}_k(\hat{\boldsymbol{\Omega}}'_*)) \log \left(\frac{f_h(\hat{\boldsymbol{\Omega}}') \check{f}_k(\hat{\boldsymbol{\Omega}}'_*)}{f_i(\hat{\boldsymbol{\Omega}}) \hat{f}_j(\hat{\boldsymbol{\Omega}}_*)} \right)$$
$$\leqslant 0. \tag{45}$$

The equal sign applies if and only if $f_i(\hat{\boldsymbol{\Omega}}) \hat{f}_j(\hat{\boldsymbol{\Omega}}_*) = f_h(\hat{\boldsymbol{\Omega}}') \check{f}_k(\hat{\boldsymbol{\Omega}}'_*)$. Now, Maxwellian distributions with equal parameters for all species are the stationary solutions of the elastic scattering terms. Inserting equation (36) into $\dot{\mathcal{H}} = 0$ and observing $\epsilon^2 = v_h^2 + v_k^2 - v_i^2 - v_j^2$ yields Boltzmann's formula as stated in equation (37).

Planck's law [3], i.e. equation (38), can be obtained from this result by inserting equation (37) into a stationary ($\partial I/\partial t = 0, I_L = 0$) and space homogeneous ($\partial I/\partial \boldsymbol{x} = 0$) version of equation (26).

5. Numerical solutions

In this section we present some numerical results of the semi-continuous model. For simplicity we confine ourselves to the case of a spatially homogeneous and isotropic gas mixture. At this level we study the impact of a monochromatic laser pulse on the shape of the distribution functions of the gas mixture. The results demonstrate the power and practical usefulness of the model.

For the numerical simulations we implement a P_0 approximation of the semi-continuous kinetic equations. This is done by means of the ansatz

$$f_i^N(\hat{\boldsymbol{\Omega}}) = \frac{1}{4\pi v_i} n_i^N. \tag{46}$$

Apart from the multiplicative constant C_χ, the quantities

$$n_i^N = v_i \int_{\mathbb{S}^2} f_i^N(\hat{\boldsymbol{\Omega}})\, \mathrm{d}\hat{\boldsymbol{\Omega}} \tag{47}$$

represent the number of particles N, $N = A, B$ and B^*, within the energy group I_i. The evolution equations for the quantities $n_i, \check{n}_i, \hat{n}_i$ and e_R are obtained by integrating equations (25*a*)–(25*c*) and (26) with respect to $\hat{\boldsymbol{\Omega}}$:

$$\frac{\mathrm{d}n_i}{\mathrm{d}t} = \mathcal{Q}_i + Q_i^{AA} + Q_i^{AB} + Q_i^{AB^*} \tag{48a}$$
$$\frac{\mathrm{d}\check{n}_i}{\mathrm{d}t} = \check{\mathcal{Q}}_i - \mathcal{S}_i + Q_i^{BB} + Q_i^{BA} + Q_i^{BB^*} \tag{48b}$$
$$\frac{\mathrm{d}\hat{n}_i}{\mathrm{d}t} = \hat{\mathcal{Q}}_i + \mathcal{S}_i + Q_i^{B^*B^*} + Q_i^{B^*A} + Q_i^{B^*B} \tag{48c}$$
$$\frac{\mathrm{d}e_R}{\mathrm{d}t} = \frac{\mathrm{d}\mathcal{S}_L}{\mathrm{d}t} - C_\chi \Delta E \sum_{i=0}^{n} \mathcal{S}_i. \tag{48d}$$

These equations form a set of coupled ordinary differential equations. Here the coupling of the gas particles with the radiation field reads $\mathcal{S}_i = \beta c e_R \check{n}_i - (\alpha + \beta c e_R)\hat{n}_i$ and the integrated collision terms are given by

$$\mathcal{Q}_i = \frac{C_\chi^2}{2}\sum_{j=0}^{n}\left\{\sum_{\substack{h,k=0\\h+k=i+j+q}}^{n}(\hat{I}_{hk}^{ij} n_h \check{n}_k - \check{I}_{ij}^{hk} n_i \hat{n}_j) + \sum_{\substack{h,k=0\\h+k=i+j-q}}^{n}(\check{I}_{hk}^{ij} n_h \hat{n}_k - \hat{I}_{ij}^{hk} n_i \check{n}_j)\right\} \tag{49a}$$

$$\check{\mathcal{Q}}_i = \frac{C_\chi^2}{2}\sum_{j=0}^{n}\sum_{\substack{h,k=0\\h+k=i+j-q}}^{n}(\check{I}_{hk}^{ij} \hat{n}_h n_k - \hat{I}_{ij}^{hk} \check{n}_i n_j) \tag{49b}$$

$$\hat{\mathcal{Q}}_i = \frac{C_\chi^2}{2}\sum_{j=0}^{n}\sum_{\substack{h,k=0\\h+k=i+j+q}}^{n}(\hat{I}_{hk}^{ij} \check{n}_h n_k - \check{I}_{ij}^{hk} \hat{n}_i n_j) \tag{49c}$$

$$\mathcal{Q}_i^{NM} = \frac{C_\chi^2}{2}\sum_{j=0}^{n}\sum_{\substack{h,k=0\\h+k=i+j}}^{n}(I_{hk}^{ij} n_h^N n_k^M - I_{ij}^{hk} n_i^N n_j^M) \tag{49d}$$

with the integrated cross sections

$$\check{I}_{ij}^{hk} = 2\pi\int_{v_0}^{v_1}\check{A}_{ij}^{hk}(v)\,\mathrm{d}v \qquad \hat{I}_{ij}^{hk} = 2\pi\int_{u_0}^{u_1}\hat{A}_{ij}^{hk}(u)\,\mathrm{d}u \qquad I_{ij}^{hk} = 2\pi\int_{-x}^{x}A_{ij}^{hk}(y)\,\mathrm{d}y. \tag{50}$$

The domains of integration (u_0, u_1), (v_0, v_1), and $(-x, x)$ coincide with the bounds of the product $\hat{\mathbf{\Omega}} \cdot \hat{\mathbf{\Omega}}_*$ as given in equation (18). The gain terms in equations (49*a*)–(49*d*) have been evaluated by exchanging the integration over pre-collisional solid angles with integration over post-collisional solid angles taking into account equations (30) and (33). The microreversibility conditions, i.e. equations (30), imply for the integrated cross sections

$$I_{hk}^{ij} = \frac{v_h v_k}{v_i v_j} I_{ij}^{hk} \qquad \check{I}_{hk}^{ij} = \frac{v_h v_k}{v_i v_j} \hat{I}_{ij}^{hk}. \tag{51}$$

In order to study relaxation phenomena, equations (48*a*)–(48*d*) are solved numerically. Due to the high speed of light, $c \approx 3 \times 10^8$ m s^{-1}, the radiation originating from emission and absorption processes of gas particles is always very close to its equilibrium value. Thus, we approximate it by Planck's law. For the calculation, we fix the following parameters: $\alpha = 10^5$ s^{-1}, $\beta = 10^7$ m^2 J^{-1}, $m = 44$ amu, $n^B + n^{B^*} = 2.5 \times 10^{22}$ m^{-3}, $\Delta E = 0.27$ eV, $\check{\sigma}(g) = 5 \times 10^{-17}$ m^3 s$^{-1}/g$. For the dominant species A we choose three different densities, namely 2.5×10^{23} m^{-3} (low density), 2.5×10^{24} m^{-3} (medium density), and 2.5×10^{25} m^{-3} (high density).

The following scenario is considered. At time $t = 0$, the gas mixture is in thermal equilibrium with the radiation field at temperature $T = 293$ K. Then a laser pulse supplies additional photons. Its intensity is given by the function $I_L(t) = I_0(t/\tau_L)\exp(-(t/\tau_L)^2)$ with $I_0 = 100$ W m^{-2} and $\tau_L = 5$ ns. A fraction of these photons is absorbed by species B yielding B^*. The excited particles B^* interact inelastically with particles A in collisional de-excitation events (cf figure 3).

The high energy released in such a process causes a distortion of the distribution functions. The actual deviation of the particle distribution functions from a Maxwellian depends critically on the assumed cross section σ and is most pronounced for species B. Figure 2 shows the distribution function of particles B at different instants of time for Maxwell molecules ($\sigma(g) = 5 \times 10^{-17}$ m^3 s$^{-1}/g$) and a low density of particles A (figure 3). The deformation can be seen best for $t = 30$ ns in figure 2.

The equivalent simulation for a hard sphere gas (diameter 3.5 Å) does not show such significant deviations from mechanical equilibrium. The reason is that for hard sphere particles

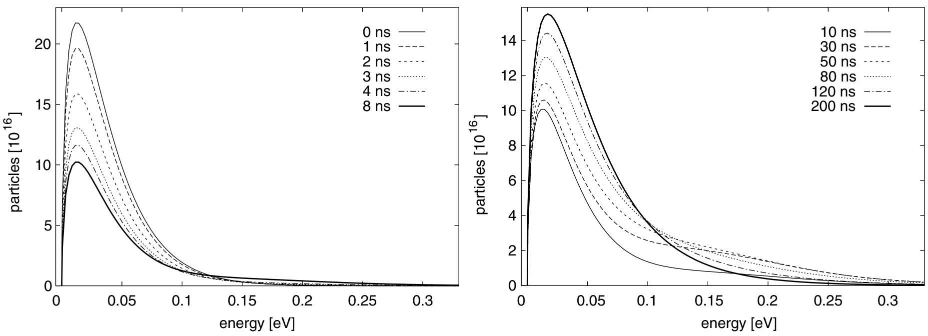

Figure 2. Evolution of species B. The left plot shows the first 8 ns where the laser pulse excites the particles and the number of B decreases. The right plot displays the re-apprearence of these particles due to inelastic collisions. Note the obvious deviation from a Maxwellian distribution.

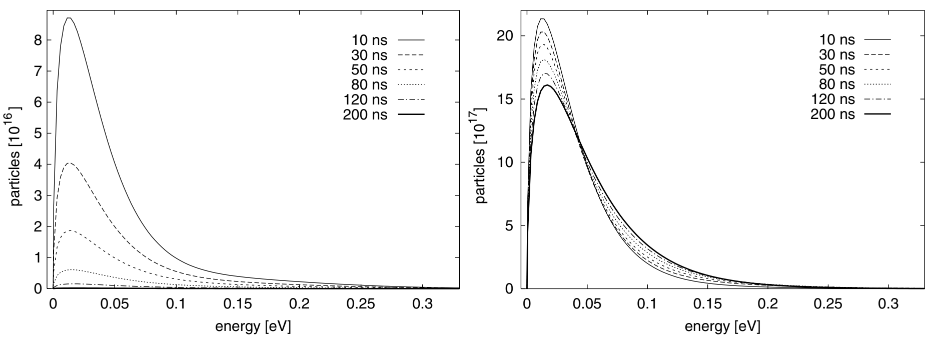

Figure 3. Evolution of species B^* (left) and species A (right). Due to de-excitation processes the number density of species B^* decreases in the course of time. The distribution of particles A is shifted towards higher energies as a consequence of the conversion of internal into kinetic energy.

the collision frequency increases with relative speed and consequently the depletion of the tails is accelerated.

On the other hand, the macroscopic quantities (excitation, energy, kinetic energy) of the gas mixture as depicted in figure 4 are relatively unaffected by the choice of the elastic cross section. The curves calculated for hard sphere molecules virtually coincide with those obtained for Maxwell molecules. The excitation is slightly smaller for hard sphere molecules because of the more efficient Maxwellization of the tails. Consequently, the laser can inject more energy into a hard sphere gas mixture (right column of figure 4) as can be seen best for a medium density of species A.

Furthermore, figure 4 illustrates how the relaxational behaviour depends on the density of particles A. A lower density of this species leads to less collisional de-excitation events per unit time and therefore greater relaxation times are observed. For the same reason, the excitation (ratio n^{B^*}/n^B) reaches much higher values for low densities of A than for high ones. In the latter case, internal energy is converted to kinetic energy much more efficiently than in the former.

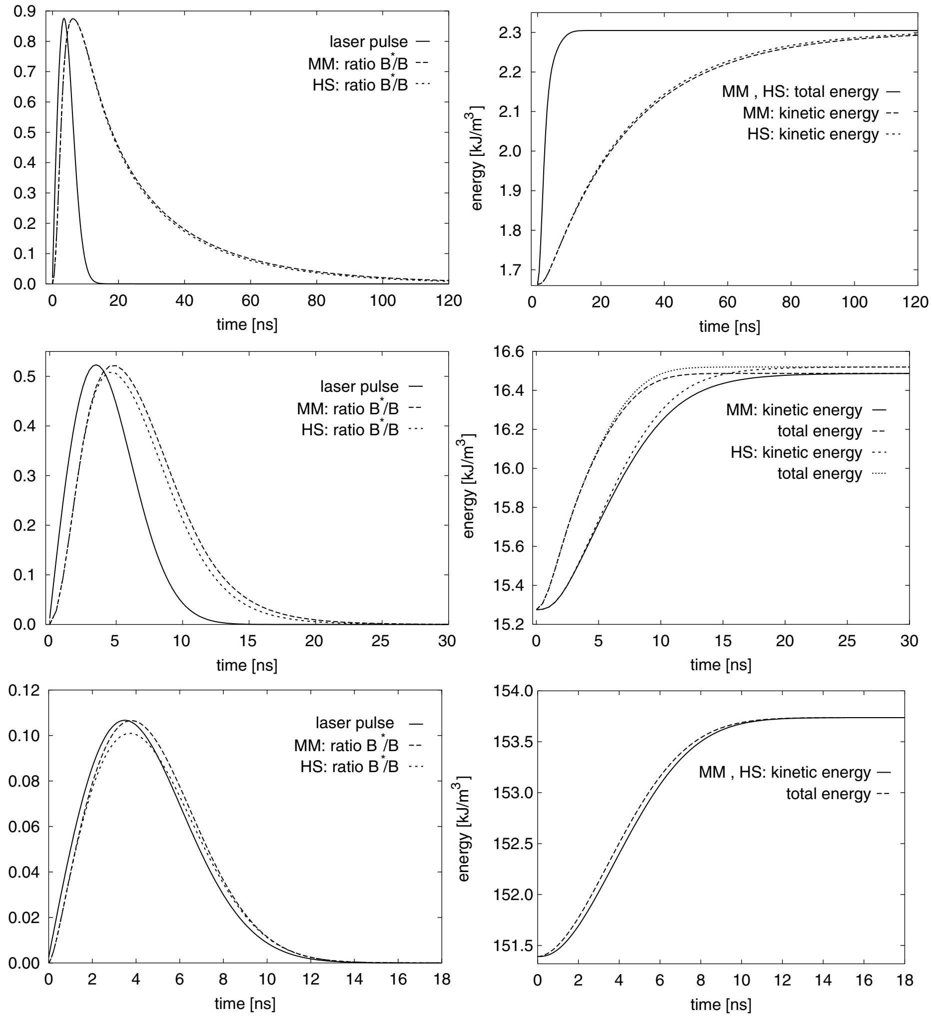

Figure 4. Temporal evolution of macroscopic quantities of the gas mixture for low density (top), medium density (middle) and high density (bottom) of species *A*. The left column shows the excitation (ratio n^{B^*}/n^B) and the intensity of the laser pulse (in arbitrary units) whereas the right column displays the evolution of the kinetic and the total energy density of the gas mixture.

6. Conclusion

We have established a semi-continuous formulation of the extended Boltzmann equations describing a gas mixture that comprises one species of structureless particles and one species of two-level atoms. By collisional excitation, the system can transfer kinetic energy to one internal degree of freedom. The interaction with monochromatic photons that can also trigger such excitation events is taken into account.

The semi-continuous model reflects the major properties (H-theorem and conservation laws) of the full continuous kinetic description. Moreover, Planck's law of radiation is recovered as the self-consistent equilibrium photon intensity.

We have applied the semi-continuous model to calculate numerically the reaction of the gas mixture to a strong coherent laser pulse. At the level of the distribution functions, we have found different degrees of deviation from Maxwellians due to fast collisional de-excitation processes. The deviations are most pronounced for the ground state of the two-level atom if the mixture is treated as Maxwell molecules. For hard spheres, only minor deviations from mechanical equilibrium are observed.

We would like to emphasize the practical usefulness of the semi-continuous model for numerical calculations. Spatially dependent simulations are scheduled as future work.

Acknowledgment

FH and WK would like to express their gratitude towards the Rector of the Graz University of Technology for a special scholarship.

References

[1] Cercignani C 1988 *The Boltzmann Equation and its Applications (Applied Mathematical Sciences 67)* (New York: Springer)
[2] Oxenius J 1986 *Kinetic Theory of Particles and Photons (Springer Series on Electrophysics 20)* (Berlin: Springer)
[3] Rossani A, Spiga G and Monaco R 1997 *Mech. Res. Commun.* **24** 237–42
[4] Garibotti C R and Spiga G 1994 *J. Phys. A: Math. Gen.* **27** 2709–17
[5] Cummings E B 1995 Laser induced thermal acoustics *PhD Thesis* California Institute of Technology, Pasadena, CA
[6] Paul P H, Farrow R L and Danehy P M 1995 *J. Opt. Soc. Am.* B **12** 384–92
[7] Hanser F, Koller W and Schürrer F 2000 *Phys. Rev.* E **61** 2065–73
[8] Bellomo N and Longo E 1991 *Math. Models Methods Sci.* **1** 113–23
[9] Preziosi L and Longo E 1997 *Japan J. Indust. Appl. Math.* **14** 399–435
[10] Reiterer P, Reitshammer C, Schürrer F, Hanser F and Eitzenberger T 2000 *J. Stat. Phys.* **98** 419–40